

We are IntechOpen, the world's leading publisher of Open Access books Built by scientists, for scientists

4,800

Open access books available

122,000

International authors and editors

135M

Downloads

Our authors are among the

154

Countries delivered to

TOP 1%

most cited scientists

12.2%

Contributors from top 500 universities



WEB OF SCIENCE™

Selection of our books indexed in the Book Citation Index
in Web of Science™ Core Collection (BKCI)

Interested in publishing with us?
Contact book.department@intechopen.com

Numbers displayed above are based on latest data collected.

For more information visit www.intechopen.com



Integrated Piezoceramics as a Base of Intelligent Actuators

Frank Bärecke, Muhammed Abed Al Wahab and Roland Kasper
*Otto-von-Guericke University Magdeburg
Germany*

1. Introduction

Embedded functionality is one main focus of technology in the upcoming century. The embedded structures are able to work as sensors and/or actuators at the same time, making a passive structure to a mechatronic device. In this chapter we focus on structures comprehending piezoceramics as actuators. Pierre and Jacques Curie discovered the piezoelectric effect in 1880. With this effect a material itself can effect a small displacement by voltage application. Only for resonance applications like speaker the reachable displacement is adequate. For most technical drive systems the reachable displacement of a piezoelectric actuator seems insufficient. This changes with the utilization of displacement amplification systems. A displacement amplification system transforms the high force but small displacement of the piezoactuator to a moderate force with useful displacement.

These displacement amplification systems are composed of passive structures of steel, polymer or ceramics and the piezoactuator itself. Basic amplification systems are bending actuators and flat leverage actuators. Bending actuators or bimorph actuators are composed of a thin piezoceramics actuator and a passive steel or ceramic plate opposite. The shrinking of the piezoceramic actuator's length by voltage application results in a bending movement allowing only very small forces. The flat leverage actuator uses the piezoactuator, the leverages and joints. Critical for these systems are the joints and the stiffness. If there is minimal backlash in one joint it will absorb the displacement of the piezo. With rising stiffness of the system the applicable force rises, but the reachable displacement will shrink.

In this chapter we give an introduction to piezoceramics, conventional piezoactuators and a new manufacturing technology. Then we focus on displacement amplification systems developed by the authors in recent years. We optimise the structures for high amplification, maximal stiffness and maximum speed of the actuator depending on the field of application. Afterwards our focus changes to two applications for amplification systems developed by the authors. Finally we discuss the capabilities of piezoceramics from the technical point of view.

2. Piezoceramics

The piezoelectric effect means the linear electromechanical interaction between the mechanical and the electrical state in crystalline materials with no inversion symmetry. An overview for sensor applications gives (Gautschi 2002) for actuator applications one can use (Janocha 2010). The direct piezo effect discovered in 1880 by Pierre and Jacques Curie

means that a structure disposed to physical loads generates a proportional charge or voltage. The direct piezoelectric effect is used for different types of sensors transforming physical loads to an electric signal. The inverse piezoelectric effect means to deform a structure by charge or voltage application. Using the inverse piezo effect the ceramics reaches a maximal elongation change of about 0.02 to 0.1 per cent of the initial length depending on the used material by an applied electric field of about 2000 V/mm. The piezoelectric (3,1)-effect or transversal effect means the extension in the direction of the field. The (3,1)-effect or longitudinal effect means a contraction orthographic to the field. The actuator has to be polarised before use in field direction. It is important not to exceed the materials Curie temperature to avoid the loss of polarisation. The actual field of application of piezoceramics comprises ink-jet printers, loud speakers, valves and diesel fuel injection systems (Janocha 2010).

Piezoactuator basics and applications

With (Ruschmeyer 1995) one can find a basic book about piezoceramics. Constitutive equations describe the piezoelectric effect of all materials using a linear model. The constitutive equations (1) and (2) represent the coupled behaviour of mechanical and electrical properties of an element, neglecting thermal or other coupling effects. On the electrical side displacement D and on the mechanical side strain S is composed of one part resulting from the electrical field E and a second part resulting from mechanical stress T

$$D = d \cdot T + \varepsilon^T \cdot E \quad (1)$$

$$S = s^E \cdot T + d \cdot E \quad (2)$$

Material data is given by electric permittivity ε , piezoelectric load constant d and mechanical compliance s . Equations (1) and (2) give constitutive equations in scalar formulation, where the electrical field and strain have the same direction, which corresponds to the (3,3)-piezoelectric effect, or are perpendicular as in the case of the (3,1)-effect. Stress and strain always have the same direction.

The constitutive equations applied to cuboids (Figure 1) with basic area A and length L , whose electrodes are supplied with a voltage $U = E \cdot L$, deliver the charge $Q = D \cdot A$ stored on that element

$$Q = d \cdot F + C \cdot U \quad (3)$$

and the change of length ΔL

$$\Delta L = \frac{F}{c_m} + d \cdot U \quad (4)$$

Here

$$F = T \cdot A \quad (5)$$

describes the force acting on the surface A , $c_m = \frac{A}{s^E \cdot L}$ specifies the spring constant and

$C = \varepsilon \cdot \frac{A}{L}$ is the capacity of the element. Eq. (5) shows how the actuator's force can be

influenced directly by adapting its area A . But eq. (4) indicates that the elongation ΔL will be small, due to the restrictions of supply voltage and the piezoelectric constant of available materials.

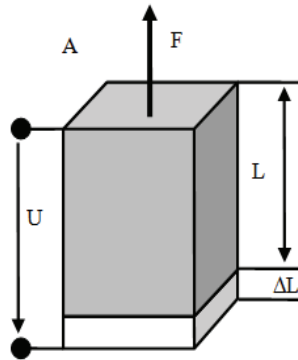


Fig. 1. Piezoelectric element

To overcome these restrictions and to generate larger motion, several construction principles of piezoactuators are common. The bender type uses the (3,1)-piezo-effect in relative long thin strips. At least two of these strips are connected together in assembly comparable to a bimetal, to get the required bending. Benders generate large motion in the mm range with the disadvantage of decreasing forces, which is the limiting factor for applications. Stack actuators use the (3,3)-piezo-effect and add the elongations of a large number of n thin elements to generate a larger motion

$$\Delta L_A = n \cdot \Delta L = \frac{F}{c_m / n} + d \cdot L_A \cdot E \quad (6)$$

As effective area A as well as the acting stress T remains unchanged, eq. (5) shows that very high forces are possible. Simply adding stacks allows only limited motions, related to the total length $L_A \approx n \cdot L$ of the actuator and suffers from a reduced stiffness of the actuator expressed by the reduced spring constant in eq. (6). Thus, in the case of stack actuators, range of motion is the limiting factor for applications. There are further actuator construction types like crossbow actuators etc. that promise a better compromise between force and motion but with the need for a more complex assembly and much higher cost.

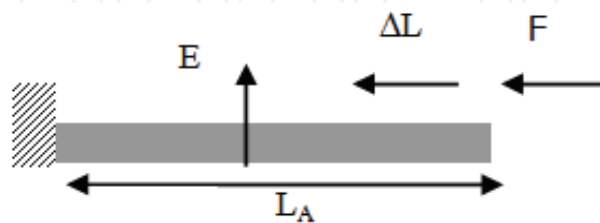


Fig. 2. Planar piezoactuator

To adapt actuator characteristics to the requirements of applications, motion amplification systems (MAS) can be used (Kasper, Heinemann und Wagner 1998), (Kasper 2002). In this paper the focus is set on mechanical solutions, as they offer a better way of integration into ceramic structures. Mechanical MAS in many cases utilize implementations of the law of lever

$$F_1 \cdot l_1 = F_2 \cdot l_2 \quad \text{und} \quad \frac{x_1}{l_1} = \frac{x_2}{l_2} \quad (7)$$

where F is force, x is motion, l is the effective lever length and index 1 means the primary, index 2 the secondary side of the lever. They offer a simple mechanical construction, but have problems with friction, backlash and stiffness. To avoid these drawbacks and to ease handling, frame constructions are used, which integrate several tasks like motion amplification, pre-stress generation and safe mounting. Unfortunately all types of MAS increase size and moved masses of the actuator. This is a contradiction to an optimized actuator system, fine tuning all its components, which is required for today's applications.

2.1 Structured actuators

Analyzing the structure of typical piezo-driven systems in order to improve integration of separated functional elements, the actuator itself and the MAS are good candidates for doing a first step. Both elements are connected by a critical interface, where very small motions have to be transmitted together with very high forces. As mentioned above, piezoelectric actuators use two principles to generate force and motion as required by an application. Benders use the (3,1)-effect to generate motion in the mm range. Due to bending the complete actuator with a very large lever arm, only forces up to 1 N can be generated. Stack actuators on the other hand use the (3,3)-effect to generate much higher forces in the range of several kN. But range of motion is restricted to 50 to 100 μm .

An alternate approach is to use the (3,1)-effect like a bender actuator to generate a large motion due to the large effective length L_A of a planar actuator. Figure 3 shows how the size of motion ΔL is determined by the actuator's length L_A and strength of the electrical field E . The necessary supply voltage therefore is given by the actuator's thickness. To reduce it, the actuator can be produced from several layers. From a practical point of view, only a small number of layers will be needed. Integrating a MAE into this planar actuator can be done in several ways. An important distinguishing feature of an MAE is the integration in the same plane as the actuator or generating motion perpendicular to this plane.

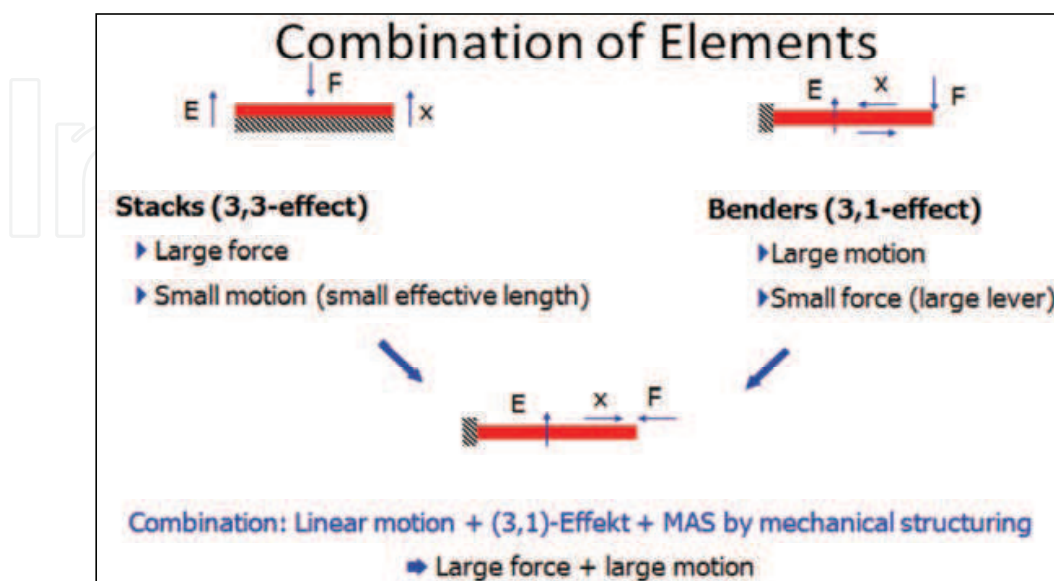


Fig. 3. Combination of Elements

Planar systems offer the advantage that all components are located in the same physical plane. As a consequence they can be produced from piezoceramic plates or discs within one structuring process. Figure 4 shows two variants of planar systems. Variant a) is driven by the length reduction of a central plate. Two levers, one on each side, amplify this motion up to $2 \times 88 \mu\text{m}$, while delivering a force of 4 N. Variant b) utilizes another method of motion amplification by adding respectively subtracting the motion generated by the bars of a meander structure.



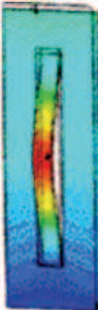
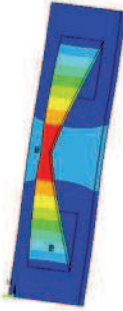
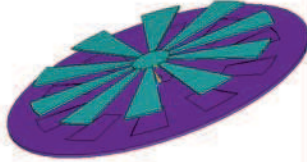
Planar Systems		Spatial Systems			
					
a) Two-sided Lever system	b) Symmetric Two-sided Meander System	c) One-sided Lever system	d) Hybrid One-sided Lever system	e) Hybrid One-sided Disc system	
2x88	2x47	64	281	511	Motion [μm]
4	0.8	1	20	40	Force [N]
70x25	70x25	70x25	70x25	$p \cdot 35^2$	Area [mm^2]

Fig. 4. Actuator prototypes using several construction principles

Variant c) uses a tongue in the middle of a base plate. If the base plate shrinks, due to an electric field, the passive tongue acts as a kind of two-side supported lever system and bends perpendicular to the base plate. Optimizing the tension distribution and designing solid joints with the aid of a FE-simulation, a motion of $64 \mu\text{m}$ can be achieved. Unfortunately forces are down on a level of 1 N. To avoid these limitations that are closely related to the solid joints used in these designs, a hybrid construction can be chosen. Variant d), which is constructed very similar to variant c), but replaces the ceramic lever by one made of spring steel, gets much better results of $281 \mu\text{m}$ motion and 20 N force. The lever will be fixed in outbreaks of the ceramic plate using special mounting elements. The strongest advantage of the hybrid type is the flexibility to adapt geometric and material data at critical points in a wider range than this can be done for a pure ceramic actuator. Variant e) shows the best results until now. More than $500 \mu\text{m}$ motion and a force of 40 N can be generated by combining a ceramic base disc with star-like MAE made of spring steel. Activating the piezoceramic disc will shrink its diameter. This radial motion is amplified and transformed to a movement of the top of the MAE perpendicular to the disc.

2.2 Synthesis of tense piezoceramic structures

Here is presented a methodology developed for synthesis of closed structures for micro- and nano-applications, utilizing the advantages of structured piezoceramics, tense

piezoactuators and closed robot kinematics structures. The synthesis of closed kinematic structure with piezoceramic actuators is investigated for three case studies:

- Synthesis for parallel structures in which the basic links are connected, only by means of driving chains of the piezoceramic actuators.
- Synthesis for parallel structures in which the basic links are connected in a serial chain. The driving chains of the piezoceramic actuators are attached parallel to the links of the basic serial chain.
- Synthesis for parallel structures in which the basic links are connected in a parallel chain. The driving chains of the piezoceramic actuators are attached parallel to the links of these chains.

A synthesis of kinematics schemes with definite degrees of freedom based on the synthesised structures is developed in the paper. The class of the kinematic joints of the links and the immovable link are selected. Examples and graphic interpretation of the solutions are presented in the paper.

Synthesis of closed structures based on piezo structured ceramics.

In order to be tensed, piezoceramic structures must be composed with parallel or closed topology. To achieve tension in closed piezoceramic structures it is possible to use predefined deformation in elastic joints or antagonistic interaction of the redundant actuators (Chakarov, et al. 2007).

Here the synthesis of basic closed structures for micro- & nano-manipulation tasks will be presented. According to the Mechanism and Machine Theory the basic closed kinematic structures include links with a number of 3, 4 or more kinematic joints, which we describe with n_j ($j \geq 3$). The following relation (Chakarov und Parushev 1994) among the number of basic links in the closed kinematic structure is used:

$$2 \cdot i = \sum_{j=3}^{i+3} (j-2) \cdot n_j \quad (8)$$

Here

$$i = p - n \quad (9)$$

is the difference between the number of the all kinematic joints p and the number of all links n in the closed kinematic chain:

$$n = \sum_{j=2}^{i+3} n_j \quad (10)$$

The possible variants of the basic links of the closed kinematic structures are derived using (8), which are presented in Table 1. In the table there are limitations on the difference (9) $i \leq 4$, and on the number n^0 of the basic links in the closed structure:

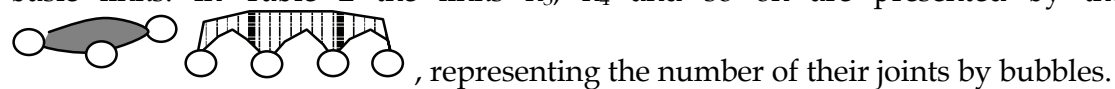
$$n^0 = \sum_{j=3}^{i+3} n_j \leq 3 \quad (11)$$

The variants of the basic links shown in Table 1 allow closed structures synthesis by means of link coupling directly among them, or by means of sequential kinematics chains including one or more links of type n_2 .

n^0	$i=1$	$i=2$	$i=3$	$i=4$
1	$n_4=1$			
2	$n_3=2$	$n_4=2$ $n_3=1, n_5=1$	$n_4=1, n_6=1$ $n_5=2$	$n_5=1, n_7=1$ $n_6=2$
3		$n_3=2, n_4=1$	$n_3=2, n_6=1$ $n_3=1, n_4=1, n_5=1$ $n_4=3$	$n_3=1, n_5=1, n_6=1$ $n_3=1, n_4=1, n_7=1$ $n_4=2, n_6=1$ $n_4=1, n_5=2$

Table 1. Possible variants of basic links of closed kinematic structures

In Table 2 are shown the possible closed structures received from Table 1, included only basic links. In Table 2 the links n_3, n_4 and so on are presented by the symbols










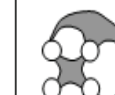




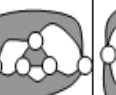
n^0	$i=1$	$i=2$			$i=3$			
1	4 							
2	3-3 	4-4 	3-5 	5-5 	4-6 			
3		3-3-4 	3-4-3 	3-6-3 	3-4-5 	3-5-4 	4-3-5 	4-4-4 

Table 2. Closed kinematic structures obtained by direct coupling of basic links

The variants of the basic links shown in Table 1 allow closed structures synthesis of link coupling by means of sequential driven kinematic chains based on piezoceramics. Piezoceramic structures can be assumed according to the Mechanism and Machine Theory as a combination of rigid links and polarised ceramic elements. The polarised ceramic elements can be estimated as actuators for linear motion, which can be modelled by the kinematic chain shown in Figure 5. It includes two links 1 and 2 and a joint T with linear motion, which can perform drive functions and two rotational joints R by which the actuator is attached to the driven links. The rotational joints can be created by introducing elastic areas in the ceramics or by additional elastic joints.

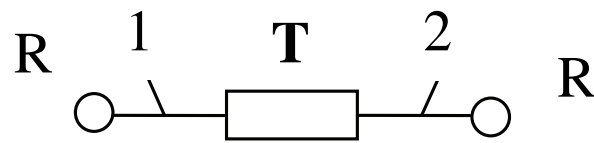


Fig. 5. Kinematic chain of linear actuator.

Three case studies of closed kinematic structure synthesis for micro- and nano-manipulation tasks

The closed kinematic structure synthesis for micro- and nano- manipulation tasks can be investigated for three case studies:

n_0	$i=0$	$i=1$	$i=2$	$i=3$	$i=4$
2	2 - 2	3 - 3	4 - 4	5 - 5	6 - 6

Table 3. Synthesised closed kinematic structures for case A)

A) Synthesis for parallel structures in which the links n_j , ($j \geq 3$) (Table 2) are connected in between, only by means of sequential kinematics chains like as driving chains clearly seen in Figure 5. The driving kinematics chains, presented in Figure 5 are sequential chains including two links from type n_2 and three joints.

The possible kinematics structures for cases $i \leq 4$ and $n^0 = 2$ defined as a result of the synthesis are shown graphically in Table 3, where the driving chains are shown by the symbol in Figure 5. The simplest closed structure 2-2 ($n_2 = 2$) can be found in Table 3, too. The number of driving chains m depends on the number of the basic links (9) and on the difference (11) as follows:

$$m = i + n^0. \quad (12)$$

B) Serial - parallel structures synthesis including the basic links n_j , ($j \geq 3$) in Table 1 connected in a serial chain that can be included and binary links n_2 . The total number n_B^0 of the links of basic serial chain includes links n_j , ($j \geq 3$) shown in Table 1 and binary links n_2 . The driving chains, presented in Figure 5 connect the free joints of the links n_B^0 of the basic serial chain in between them. A restriction is imposed for structures synthesis only including number m of the driving chains higher than the number of the joints connecting the links of the serial chain. The reason for this restriction is the fact that all the joints of the basic serial chain are driven by means of parallel driving chains. The kinematics structures defined as a result of synthesis for $n^0=1, 2$ according to Table 1 are shown graphically in Table 4 on the left side. In Table 4 the possible kinematic structures are shown for case $i \leq 2$ and the number of the links of basic serial chain $n_B^0 = 2, 3$. The number of the driving chains m in this case is defined by i in equation (9):

$$m = i + 1. \tag{13}$$

Here, the same graphical symbols as in Table 3 are used for the link and the driving chain definition. The difference in the arrangement of the links in Table 2 is also assessed. The simplest closed structure $n_2 = 2$ is shown in Table 4, too.

C) Parallel structures synthesis including the basic links $n_j, (j \geq 3)$ in Table 1 connected in between in a parallel chain that can be included and binary links n_2 . The total number n_B^0 of the links of the basic parallel chain includes links $n_j, (j \geq 3)$, shown in Table 1, and binary links n_2 .

The driving chains (Figure 5) connect the free joints of the links n_B^0 of the basic parallel chain in between them. The number of the driving chains in this case is defined by the difference (9) as: $m = i$.

The kinematic structures defined as a result of synthesis for $n^0 = 2, 3$ and $i = 1, 2$ according Table 1 are shown graphically in Table 4 on the left. On the right of Table 4 the possible kinematic structures are shown for case $i = 1, 2$ and the number of the links of basic parallel chain $n_B^0 = 3$.

n_B^0	$i=0$	$i=1$	$i=2$		n_B^0	$i=1$	$i=2$
2	2-2 	3-3 	4-4 			3-3 	4-4
3		3-2-3 	4-2-4 		3		3-3-4
		2-3-3 	2-4-4 	3-3-4 			3-4-3
		2-4-2 	2-5-3 	3-4-3 			

Table 4. Synthesised closed kinematic structures for case B) and for case C)

Synthesis of kinematics schemes for micro- & nano-manipulation tasks based on the synthesised structures.

A synthesis of kinematics schemes with definite degrees of freedom h based on the synthesised structures can be developed. To create the kinematics schemes with definite degrees of freedom, the class j of the kinematics joints p_j of the links and the immovable link are selected. The synthesis is performed separately for case A), B) and C) about structures of Tables 3 and 4.

A) For parallel structures of Table 3 the number of the degrees of freedom usually is equal to the number of the actuators $h = m$. If the number of the actuators m is larger than that of the degrees of freedom $m \geq h$ we have actuation redundancy. This can be used for achieving the tensility, improving the dynamic parameters and removing any backlash in the device. The redundancy is presented by the difference:

$$m - h = r. \quad (14)$$

To create the kinematics schemes with definite degrees of freedom, the class j of the kinematic joints p_j of the links has to be selected. The number and the class of the kinematics joints are defined by the actuators. Each actuator according to Figure 5 possesses one linear motor joint (T) and two revolution joints (R). The linear joints apply 5 restrictions to the movements, thus the joint possess one degree of freedom. Their number p_5^l is equal to the number of the actuators:

$$p_5^l = m. \quad (15)$$

The revolution joints of the parallel structures of Table 3 can apply different number of restriction $j = 1..5$, defining the degrees of freedom of the device using the well known equation:

$$h = 6 \cdot n - \sum_{j=1}^5 j \cdot P_j \quad (16)$$

where n is the number of all mobile links and P_j is the number of all kinematics joints of class j .

As any actuator has two movable links and one of the basic links n^0 is immovable, the number of all mobile links is:

$$n = n^0 - 1 + 2 \cdot m. \quad (17)$$

As the number of all kinematics joints of class $j=5$ includes the number of linear joints p_5^l and the number of revolution joints p_5^r of class 5 according (15) it leads to:

$$P_5 = p_5^l + p_5^r = m + p_5^r. \quad (18)$$

According (17) and (18) equation (16) assumes the form:

$$h = 6 \cdot (n^0 - 1) + 7 \cdot m - \sum_{j=1}^5 j \cdot p_j^r. \quad (19)$$

As any actuator according Figure 5 has two revolution joints, the total number of revolution joints is defined by the number of actuators m :

$$\sum_{j=1}^5 p_j^r = 2 \cdot m. \quad (20)$$

For any structural scheme of Table 3 defined by parameters n^0 and i ($i=m+n^0$), above two equations (19) and (20) allow to determine one or more variants of allocation of the different class joints and synthesis of kinematics schemes with desired degrees of freedom $h = m - r$. If we use elastic revolution joints (geometric closed), the class of joints is limited $j = 3, 4, 5$. The possible revolution joints p_j^r according equations (19) and (20) for structures of Table 3 ($n^0=2$) with $h=1,2,3$ and $i=0, \dots, 4$ are shown in Table 5.

h	i=0, m=2	i=1, m=3	i=2, m=4	i=3, m=5	i=4, m=6
1	$p_4=1, p_5=3$	$p_4=4, p_5=2$ $p_3=1, p_4=2, p_5=3$ $p_3=2, p_5=4$	$p_4=7, p_5=1$ $p_3=1, p_4=5, p_5=2$ $p_3=2, p_4=3, p_5=3$ $p_3=3, p_4=1, p_5=4$	$p_4=10$ $p_3=1, p_4=8, p_5=1$ $p_3=2, p_4=6, p_5=2$ $p_3=3, p_4=4, p_5=3$ $p_3=4, p_4=2, p_5=4$ $p_3=5, p_5=5$	$p_3=1, p_4=11$ $p_3=2, p_4=9, p_5=1$ $p_3=3, p_4=7, p_5=2$ $p_3=4, p_4=5, p_5=3$ $p_3=5, p_4=3, p_5=4$ $p_3=6, p_4=1, p_5=5$
2	$p_3=1, p_5=3$	$p_4=5, p_5=1$ $p_3=1, p_4=3, p_5=2$ $p_3=2, p_4=1, p_5=3$	$p_4=8$ $p_3=1, p_4=6, p_5=1$ $p_3=2, p_4=4, p_5=2$ $p_3=3, p_4=2, p_5=3$ $p_3=4, p_5=4$	$p_3=1, p_4=9, p_5=2,$ $p_4=7, p_5=1$ $p_3=3, p_4=5, p_5=2$ $p_3=4, p_4=3, p_5=3$ $p_3=5, p_4=1, p_5=4$	$p_3=2, p_4=10$ $p_3=3, p_4=8, p_5=1$ $p_3=4, p_4=6, p_5=2$ $p_3=5, p_4=4, p_5=3$ $p_3=6, p_4=2, p_5=4$ $p_3=7, p_5=5$
3	X	$p_4=6$ $p_3=1, p_4=4, p_5=1$ $p_3=2, p_4=2, p_5=2$	$p_3=1, p_4=7$ $p_3=2, p_4=5, p_5=1$ $p_3=3, p_4=3, p_5=2$ $p_3=4, p_4=1, p_5=3$	$p_3=2, p_4=8, p_5=3,$ $p_4=6, p_5=1$ $p_3=4, p_4=4, p_5=2$ $p_3=5, p_4=2, p_5=3$ $p_3=6, p_5=4$	$p_3=3, p_4=9$ $p_3=4, p_4=7, p_5=1$ $p_3=5, p_4=5, p_5=2$ $p_3=6, p_4=3, p_5=3$ $p_3=7, p_4=1, p_5=4$

Table 5. The possible revolution joints for case A)

B) Serial - parallel structures of Table 4 (left side) allow the basic serial chain to determine the degrees of freedom of the device h . The joints of this chain can be elastic and can bear the necessary motion restrictions. The actuators are treated as identical structural groups with zero degrees of freedom (Figure 6). The class of the rotation joints of the actuators are chosen in such a way according to (16), do not change the degrees of freedom of the basic chain. The class of the rotation joints for the spatial (3D) case are shown in Figure 6.

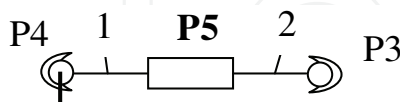


Fig. 6. Class of the actuator joints for the spatial (3D) case

The number of the actuators usually is equal to the number of the degrees of freedom $m=h$. If the number of the actuators m is larger than that of the degrees of freedom $m \geq h$ we have actuation redundancy presented through difference (14). This can be used for achieving the tensity, improving the dynamic parameters and removing the backlashes in the device.

The class of the joints of the basic serial chain is determined according equation (16) presented as:

$$h = 6 \cdot (n_B^0 - 1) - \sum_{j=1}^5 j \cdot p_j^0 \tag{21}$$

where n_B^0 and p_j^0 are the number of the links and the joints of the basic serial chain. The joints number of the basic serial chain is determined according the number of its movable links using equality:

$$n_B^0 - 1 = \sum_{j=1}^5 p_j^0 . \quad (22)$$

For each structure of Table 4 with desired degrees of freedom h , above two equations (21) and (22) allow determining the class of basic chain joints and their number. If the class of revolution joints is limited $j = 3, 4, 5$, the possible joints p_j of the basic serial chain with $h=1, 2, 3, 4, 5$ degrees of freedom and $n_B^0 = 2, 3$ are shown in Table 6.

H	1	2	3	4	5
$n_B^0 = 2$	$p_5=1$	$p_4=1$	$p_3=1$	X	X
$n_B^0 = 3$	X	$p_5=2$	$p_4=1, p_5=1$	$p_4=2$	$p_3=1, p_4=1$

Table 6. The possible joints p_j of the basic serial chain

Each basic joint of class j must be included in $(6-j)$ closed cycles with the actuators of structure to get the drivability. The joints with definite class of the basic chain can be either revolution or linear, as well.

C) In the parallel structures of Table 4 (right side) the actuators are treated too as identical structural groups with a zero degrees of freedom (Figure 6). The basic parallel chain determines the degrees of freedom of the device h . The number of the actuators is equal to the number of the degrees of freedom $m = h$, or it is larger of them $m > h$. The class of joints p_j^0 of the basic parallel chain is defined by equation (16) as:

$$h = 6 \cdot (n_B^0 - 1) - \sum_{j=1}^5 j \cdot p_j^0 . \quad (23)$$

where n_B^0 and p_j^0 are the number of the links and the joints of the basic parallel chain. The total number of the joints of the basic parallel chain is equal to the number of its links:

$$n_B^0 = \sum_{j=1}^5 p_j^0 . \quad (24)$$

Above two equations allow for each structure of Table 5 (right side) included n_B^0 links, to specify the class of the joints of the basic parallel chain with h degrees of freedom. If the class of elastic revolution joints is limited $j = 3, 4, 5$, the possible solutions for structures with $h=1, 2, 3, 4, 5$ degrees of freedom and $n_B^0=3, 4$ are shown in Table 7.

h	1	2	3	4	5
$n_B^0 = 3$	$p_3=1, p_4=2$	$p_3=2, p_4=1$	$p_3=3$	X	X
	$p_3=2, p_5=1$				
$n_B^0 = 4$	$p_3=1, p_4=1, p_5=2$	$p_3=1, p_4=2, p_5=1$	$p_3=2, p_4=1, p_5=1$	X	X

Table 7. The possible joints p_j of the basic parallel chain

3. Integrated displacement amplification system examples

The first and the second example show two displacement amplification systems for very precise positioning in 3D. The aim was to synthesize a mechatronic handling device with 3 degrees of freedom – two degrees affect the orientation the third affects the translation. The amplification system is appropriate for cell manipulation. For this purpose two prototypes were experimentally investigated utilizing the synthesized kinematic structures based on cases A) and B).

The development of an adaptive Gas-Spring-Damper System (GSD) resulted in a need for a very fast high flow pneumatic fluid restrictor. The appropriate application area of an adaptive Gas-Spring-Damper is a passenger cars suspension strut. Other possible application areas are seat or cabin dampers. GSDs comprises mostly of two or three air chambers with different working directions. A fluid restrictor connects these air chambers. The GSD behaviour as a spring and damper system depends on geometries of the air chambers and the air flow controlled by the fluid restrictor. For the development of an adaptive GSD one requires a variable fluid restrictor for controlling the damping mode of it. The second example presents the fluid restrictor and the integrated piezoelectric displacement amplification system developed for controlling the GSDs gas flow. The displacement amplification system comprises a piezoceramic ring, where the piezoelectric (3,1)-effect is used, and spokes which connect the ring to an inner bearing. To improve the amplification we designed several structures which differ in spoke thickness, material and position. Alteration of the piezo design does not seem promising. Plungers extend the spokes for sealing the long holes embedded in the housing, enabling building up a fluid restrictor from the displacement amplification system. The third example shows the integration of the displacement amplification in a pneumatic fluid restrictor.

3.1 Mechatronic handling device with three piezoelectric actuators

The mechatronic handling device is based on the kinematic structure with two links of the basic serial chain $n_B^0 = 2$ (structure type of case B)) and three degrees of freedom $h=3$. The number of the actuators is equal to the number degrees of freedom of the device $m = h = 3$. According to equation (13) and Table 4 (left side), structure 4-4 corresponds to the chosen parameters. The structure is symmetric and each basic link can be chosen as an immovable one as it is shown in Figure 7 a). Following equations (21), (22) and results in Table 6, the possible joints distribution of the basic serial chain is $p_3=1$. On the above it can be build up a kinematics scheme of a device for micro- and nano-manipulation tasks as shown in Figure

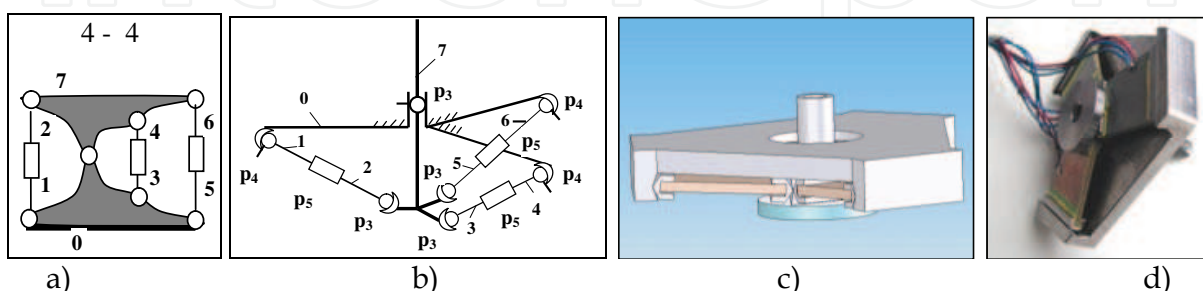


Fig. 7. Development of the handling device with structured piezoceramics (type B) with $n_B^0 = 2$ and $h=m=3$

7b). Actuator chains in the scheme are chosen according Figure 6. The basic chain includes two links marked as 0 and 7, connected by means of one elastic joint p_3 , allowing one linear and two rotational movements. Link 0 is chosen as immovable one. Based on this scheme a simulation model (Figure 7 c) and a device prototype (Figure 7.d) with structured piezoceramics are developed. (Kasper, Al Wahab, et al. 2006)

3.2 Mechatronic handling device with six piezoelectric actuators

It is based on the kinematic structures with two links of the basic serial chain $n_0=2$ (structure type A) and three degrees of freedom $h=3$. The number of the actuators is 3 and therefore bigger than the number of degrees of freedom of the device, as follows: $m = h+r = 3+3 = 6$. According equation (12) and Table 4 (left side) structure 6-6 corresponds to the chosen parameters. The structure is symmetric and each basic link can be chosen as immovable one as it is shown in Figure 7 a). Based on the equations (21) and (22) and results in Table 6, the possible revolution joints distributions are the following:

$p_3=3, p_4=9$; $p_3=4, p_4=7, p_5=1$; $p_3=5, p_4=5, p_5=2$; $p_3=6, p_4=3, p_5=3$ and $p_3=7, p_4=1, p_5=4$.

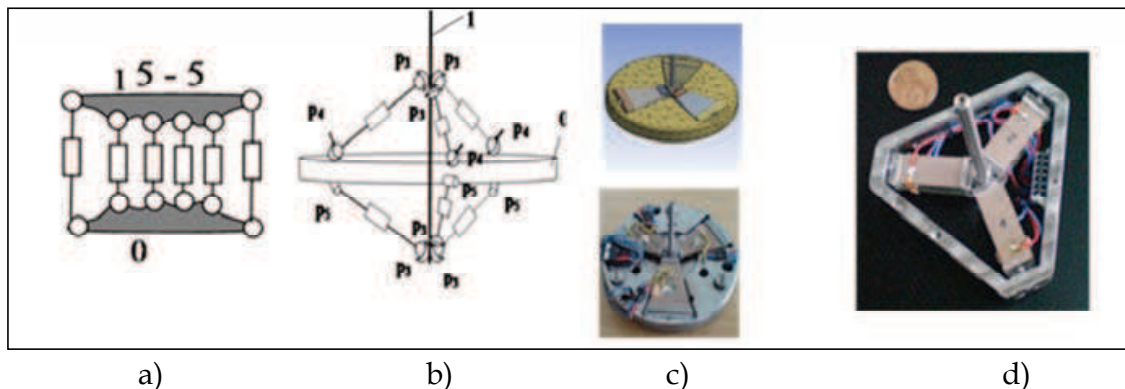


Fig. 8. Phases of design during development of the handling device with structured piezoceramics (type A) with $n_0=2$ and $h=3$, $m=6$.

In this case a kinematics scheme with joints $p_3=6, p_4=3, p_5=3$, is chosen as it is shown on Figure 7 b). Actuator chains in the scheme are chosen according to Figure 6. The basic two links are indicated as 0 and 1, while link 0 is chosen as the immovable one. A simulation model and a device prototype with structured piezoceramics built up that scheme are shown on Figure 8 c) and d).

3.3 Air flow restrictor

The requirements of the fluid restrictor are speed and high flow rate to be able controlling the GSD damping mode. In most operational mode the pressure difference between the air chambers is small and depends in particular on the stimulation of the road. It can vary between a few Pa and some bar for extreme road unevenness at high speed. The operational pressure for a GSD application lies between 5 and 20 bars. Restrictions are here the overall size, which rises with decreased pressures, and the technology to provide the compressed air. Due to the application area the fluid restrictor must resist all shocks caused by road unevenness (Bärecke, Kasper und Al Wahab 2008) and (Kasper, Bärecke, et al. 2008).

Displacement amplification system

The displacement amplification system comprises a piezoceramic ring (Figure 9 and Figure 10). Voltage application on the piezoelectric actuator causes it to enlarge in thickness.

The piezoelectric (3,1)-effect causes a contraction of the ring and coincidental reduces its diameter. Six spokes connect an inner bearing to the piezoceramic ring. They can't contract like the piezoceramic ring due to their high longitudinal stiffness. This leads them to bend. This results in an angular movement of the actuator and a rotation on the outside of the piezoceramic ring. Important influencing factors for the displacement amplification are the adjustment, and thickness of the spokes. Thicker spokes have a higher bending stiffness, so they are working against the rotation, therefore decreasing the maximum amplification. For maximum displacement amplification one can reduce the eccentricity, but on the other hand this reduces the operational torque.

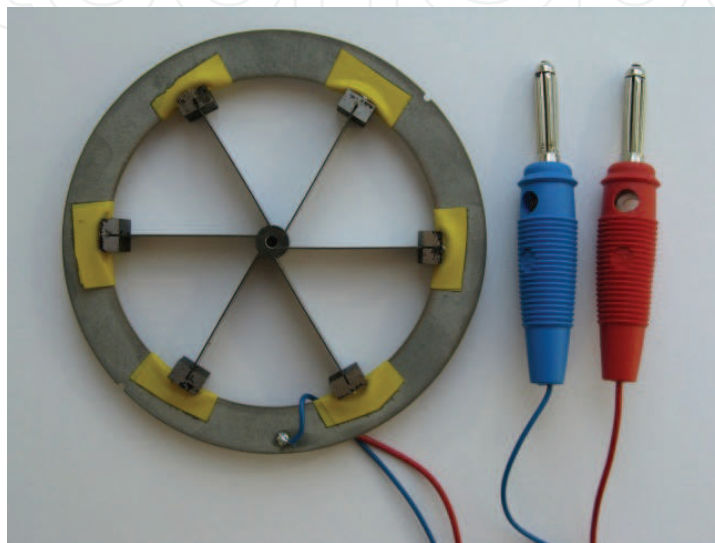


Fig. 9. Discrete displacement amplification prototype

Figure 9 shows an early prototype for the displacement amplification system. The piezoelectric ring is cut out of a quadratic plate by jet cutting. Bearings and spring steel spokes are eroded from a steel block. This amplification system is manually assembled. The amplification system has a diameter of about 80 mm. The piezoelectric actuator is 1.5 mm, the spokes are 0.4 mm thick and have an eccentricity of 0.8 mm. To avoid electrical breakdown between the piezoceramics ring and the bearing resides adhesive tape. The measured displacement of this prototype is 0.45 mm.

The left side of Figure 10 shows a prototype manufactured with the technology of insert moulding. A carbon fibre polymer is mould over the piezoceramic ring. This prototype reaches a displacement of about 0.3 mm. The right part of that Figure shows a FEM simulation for this amplification system. The results of the simulation and the measured values are about the same size. This could be aroused by geometry meanderings like draft angle due to the moulding process. The insert moulded spokes have a trapezoid format which is need for the demoulding process.

Further development of the displacement amplification system

Calculations showed that the needed amplification wasn't reached by these first prototypes. An improved amplification system has to be developed. To reduce the restoring force of the bended spokes thinner spokes have to be used. It is possible to use spring steel inlays with a thickness of 0.3 mm or even thinner dimension. Insert moulded spokes have a boundary for spokes thickness at about 0.5 mm. Thinner spokes could clog the capillary of the moulding

form which is handled by an increased moulding pressure. This increased moulding pressure degrades the piezoceramics so we can't use it. In summary with spring steel inlays we could decrease injection pressure and rejection rate due to broken piezoceramics.

The left of Figure 11 shows a displacement amplification system with spring steel inlays. The spring steel spokes are connected by insert moulding to the inner bearing. Outer bearings connect the spring steel inlays to the piezoceramic ring. The spring steel inlays ends are rounded by brazing to prevent them cutting the carbon polymer. The moulding process has to fill seven independent cavities. The right of Figure 11 shows the mounting position of the displacement amplification system. It is arranged in a housing containing six outlet notches of 1x10 mm. In the closed position discs at the end of the displacement amplification system cover the outlet notches. With an applied voltage the ring rotates and a voltage proportional air flow crossing area is uncovered. The valve additionally incorporates six areas of air flow with an approximate crossing section of 0.7x10 mm. Very important for the use of the fluid restrictor in the GSD is the leakage of the closed restrictor. The circumferential line surrounding all outlet notches is proportional to the leakage. The additional length of this parameter is 130 mm. It was calculated, that a leakage minimization is possible with a production accuracy of about 10 μm .

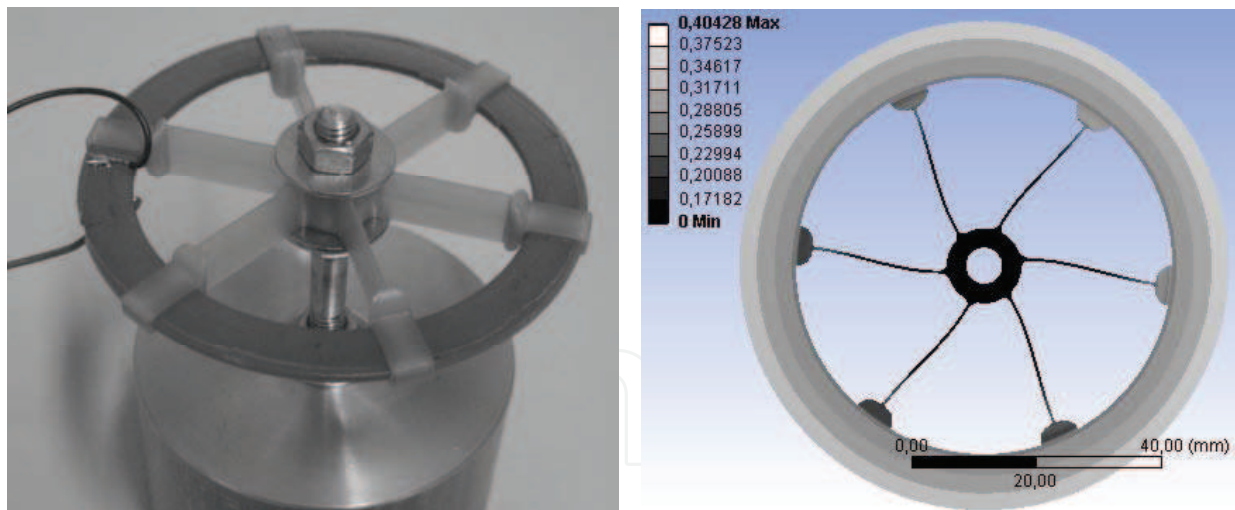


Fig. 10. Displacement amplification system made by insert moulding (left), displacement amplification system FEM simulation results (right)

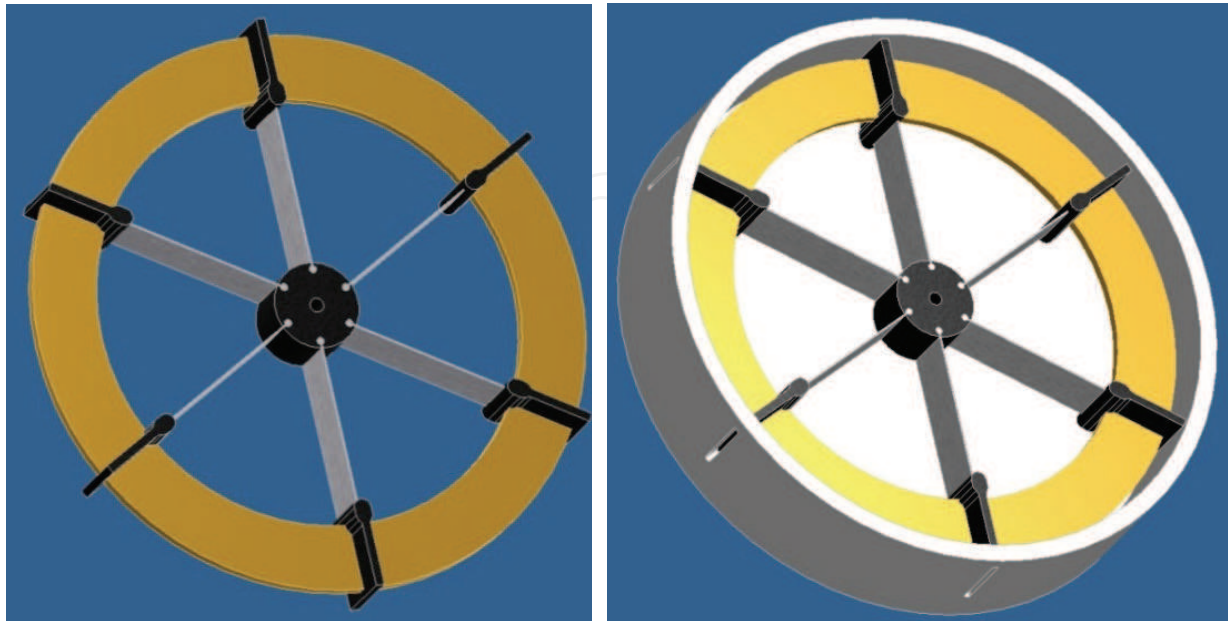


Fig. 11. Improved displacement amplification System using steel spokes (left), fluid restrictor with improved displacement amplification system (right)

Actuator	Displacement μm	Maximal moment Nm	First eigen frequency Hz
Discrete	410	6	248
Insert moulding	400	0,18	121
New 1.0	470	0,54	197
New 0.8	570	0,44	155
New 0.7	630	0,38	144
New 0.6	710	0,33	129

Table 8. Displacement amplification for miscellaneous actuators

Table 8 illustrates a comparison of different types of displacement amplification systems: The discrete amplification system shown in Figure 9, the first insert moulding prototype shown on the left side of Figure 10 and the first improved amplification system (New 1.0) shown in Figure 11 are similar with respect to the maximum displacement. This results from the constant eccentricity of the spokes of one mm. From these the discrete prototype using only steel as bearing and spokes provides the maximal torque. The new amplification system has a tripled force compared with the first insert moulding prototype and also improves the amplification. Varying the spokes eccentricity down to 0.6 mm with the new displacement amplification system allowed us improving the displacement further up to over 700 μm . With a restoring force of the previous actuator it had to overbear this was not possible. This force is proportional to the second moment of area of the spokes which rises with the third order of the spokes thickness. The Figure shows the first natural frequency of the actuator in addition. This should be higher than 100Hz for our application; all actuators achieve that. The higher eigenfrequencies of the amplification systems are all above 1000 Hz. With the example of the air flow restrictor one can see the benefits of the integration of different materials in one displacement amplification system. Therefore a sophisticated manufacturing technology like piezoceramic injection moulding and piezoceramic insert moulding is needed.

Piezoceramic manufacturing technology

The main common shaping process of piezoceramics is isostatic dry pressing, where powder granulate is pressed into the form. The slip casting is used for producing thin foils with controllable tolerances. These technologies have an issue with complex geometries. These complex geometries are needed for the integrated amplification systems. Therefore a new shaping technology for piezoceramics is needed.

A new shaping process of piezoceramics is the Ceramic Injection Moulding (CIM), which is a manufacturing technology that allows generating very complex structures of piezoceramics. For this process the PZT-powder is mixed with a thermoplastic binder system to a feedstock, which can be moulded at a temperature of 160°C. The required moulding tool that includes the three-dimensional cavity for the actuator has to be designed in CAD considering the materials shrinking behaviour on later process steps. To avoid incomplete filling one simulates the filling process with the CAD-model of the filling cavity under consideration of material properties. In general melt fronts due to different injection points for one cavity have to be avoided in the CIM process, because of the appearance of entrapments when the part gets sintered. After the forming, the binder system must be removed by thermal treatment. To compact the piezo grain structure one sinters the piezoceramic actuator at 1300°C. Next process steps were the metallization, which is done by sputtering and polarization with 4 kV per one millimetre thickness at 90°C. While the thermal disposal of the binder and the sintering process the actuator shrinks. This allowance must be reminded while designing the cavity for the actuator. The ceramic injection moulding process can be used for all of the actuators in the displacement amplification systems getting geometric optimized actuators.

Ceramic injection moulding supersedes finishing treatment of the actuator preparing it for its use in the amplification system. For early prototypes one can use water jet cutting for two dimensional processing. Here the ceramic plate is glued with thermal glue on a metal plate, preventing it from breaking while water jet cutting. Afterwards it is heated and separated

from the metal plate. One has to observe using thermal glue with lower melting point than the curie temperature of the piezoceramic actuator.

Another possible finishing technology is laser cutting. A high energy laser is needed which gives only a very short energy impulse avoiding depolarisation. Ultrasonic manufacturing is also possible with moderate costs. With ultrasonic manufacturing the ceramic could break due to the finishing process. For a large scaled amount of actuators these finishing processes are too expensive.

5. Conclusion

This chapter gave a short introduction to piezoceramics. Starting from flat and bending actuators with the need for moderate force and displacement at the same time, structured actuators were introduced. The structured amplification systems started from flat ones, went on with lever systems and finished with three examples of complex amplification systems. While the first amplification system is only from piezoceramics, the later ones integrate steel gaining more force and displacement amplification. The last amplification system integrates additional carbon fibre polymer. This allows an integrated manufacturing process and increases displacement amplification.

6. Acknowledgment

The research work of the authors is supported by the European Regional Development Fund (EFRE).

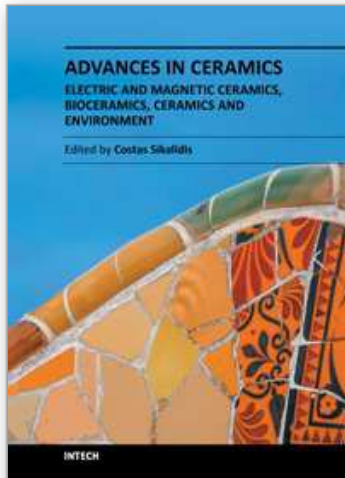
7. References

- Bärecke, F, R Kasper, und M Al Wahab. „A structured piezo ceramic valve for an adaptive car gas damping system.“ 5th International Symposium on Mechatronics and its Applications ISMA. Amman, Jordan: IEEE, 2008.
- Chakarov, Dimitar, Muhammed Al Wahab, Roland Kasper, und Kostadin Kostadinov. „Synthesis of tense piezo structures for local micro- and nano manipulations.“ 8. Magdeburg Maschinenbautage & 7. Mahreg Innovationsforum. Magdeburg: Universität Magdeburg, 2007. 173-180.
- Gautschi, G. Piezoelectric Sensorics. Berlin Heidelberg: Springer Verlag, 2002.
- Janocha, H. Unkonventionelle Aktoren. München: Oldenburg, 2010.
- Kasper, R. „Mechatronisches Design integrierter Piezoaktoren.“ ISOM 2002 "Innovative Antriebstechnik". Chemnitz, 2002. 379-392.
- Kasper, R, F Bärecke, M Al Wahab, M Harmann, und Matthias Hartmann. „High flow piezo ceramic valve for an adaptive vehicle gas spring damper.“ Actuator 2008. Bremen, 2008. 927-930.
- Kasper, R, M Al Wahab, W Heinemann, K Kostadinov, und D Chakarov. „Mechatronic handling device based on piezo ceramic structures for micro and nano applications.“ Actuator 2006. Bremen, 2006. 154-158.
- Kasper, R, W Heinemann, und A Wagner. „Modelling and Control for Piezoelectric Actuators for high speed applications.“ Movic. Zürich, 1998. 231-236.

Ruschmeyer, Karl. Piezokeramik: Grundlagen, Werkstoffe, Applikationen. Renningen-Malmsheim: expert-Verlag, 1995.

IntechOpen

IntechOpen



**Advances in Ceramics - Electric and Magnetic Ceramics,
Bioceramics, Ceramics and Environment**

Edited by Prof. Costas Sikalidis

ISBN 978-953-307-350-7

Hard cover, 550 pages

Publisher InTech

Published online 06, September, 2011

Published in print edition September, 2011

The current book consists of twenty-four chapters divided into three sections. Section I includes fourteen chapters in electric and magnetic ceramics which deal with modern specific research on dielectrics and their applications, on nanodielectrics, on piezoceramics, on glass ceramics with para-, anti- or ferro-electric active phases, of varistors ceramics and magnetic ceramics. Section II includes seven chapters in bioceramics which include review information and research results/data on biocompatibility, on medical applications of alumina, zirconia, silicon nitride, ZrO₂, bioglass, apatite-wollastonite glass ceramic and b-tri-calcium phosphate. Section III includes three chapters in applications of ceramics in environmental improvement and protection, in water cleaning, in metal bearing wastes stabilization and in utilization of wastes from ceramic industry in concrete and concrete products.

How to reference

In order to correctly reference this scholarly work, feel free to copy and paste the following:

Frank Bärecke, Muhammed Abed Al Wahab and Roland Kasper (2011). Integrated Piezoceramics as a Base of Intelligent Actuators, *Advances in Ceramics - Electric and Magnetic Ceramics, Bioceramics, Ceramics and Environment*, Prof. Costas Sikalidis (Ed.), ISBN: 978-953-307-350-7, InTech, Available from:

<http://www.intechopen.com/books/advances-in-ceramics-electric-and-magnetic-ceramics-bioceramics-ceramics-and-environment/integrated-piezoceramics-as-a-base-of-intelligent-actuators>

INTECH
open science | open minds

InTech Europe

University Campus STeP Ri
Slavka Krautzeka 83/A
51000 Rijeka, Croatia
Phone: +385 (51) 770 447
Fax: +385 (51) 686 166
www.intechopen.com

InTech China

Unit 405, Office Block, Hotel Equatorial Shanghai
No.65, Yan An Road (West), Shanghai, 200040, China
中国上海市延安西路65号上海国际贵都大饭店办公楼405单元
Phone: +86-21-62489820
Fax: +86-21-62489821

© 2011 The Author(s). Licensee IntechOpen. This chapter is distributed under the terms of the [Creative Commons Attribution-NonCommercial-ShareAlike-3.0 License](#), which permits use, distribution and reproduction for non-commercial purposes, provided the original is properly cited and derivative works building on this content are distributed under the same license.

IntechOpen

IntechOpen